Science of the Total Environment 706 (2020) 134978

Contents lists available at ScienceDirect

Science of the Total Environment

journal homepage: www.elsevier.com/locate/scitotenv

Forecasting emergency admissions due to respiratory diseases in high variability scenarios using time series: A case study in Chile

Miguel Becerra [a], Alejandro Jerez [a,*], Bastián Aballay [a], Hugo O. Garcés [b], Andrés Fuentes [a]

[a] Departamento de Industrias, Universidad Técnica Federico Santa María, Av. España 1680, Casilla 110-V, Valparaíso, Chile
[b] Computer Science Department, Universidad Católica de la Santísima Concepción, Alonso de Ribera 2850, Concepción 4090541, Chile

HIGHLIGHTS

- Fulfillment emergency admissions due respiratory diseases is challenging in winter season.
- Exploratory data analysis and hyperparameters grid search was implemented.
- SARIMA modelling is an adequate modelling approach for Chilean time series.
- MAPE is under 20% considering 30-day ahead forecasting process.
- Improvement hospital resource management eases dealing with admission variability.

GRAPHICAL ABSTRACT

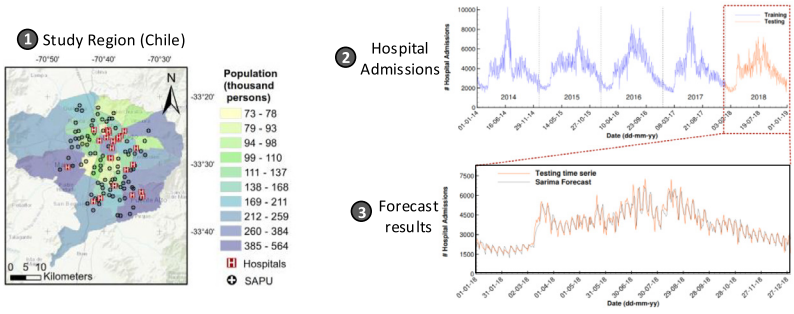

ARTICLE INFO

Article history:
Received 21 July 2019
Received in revised form 12 October 2019
Accepted 13 October 2019
Available online 23 November 2019

Editor: Scott Sheridan

Keywords:
Time series
Emergency admissions
Respiratory diseases
Forecasting
Hospital management
SARIMA

ABSTRACT

Respiratory diseases are ranked in the top ten group of the most frequent illness in the globe. Emergency admissions are proof of this issue, especially in the winter season. For this study, the city of Santiago de Chile was chosen because of the high variability of the time series for admissions, the quality of data collected in the governmental repository DEIS (selected period: 2014–2018), and the poor ventilation conditions of the city, which in winter contributes to increase the pollution level, and therefore, respiratory emergency admissions. Different forecasting models were reviewed using the Akaike Information Criteria (AIC) with other error estimators, such as the Root Mean Square Error (RMSE), for selecting the best approach. At the end, Seasonal Autoregressive Integrated Moving Average (SARIMA) model, with parameters $(p,d,q)(P,D,Q)_s = (2,1,3)(3,0,2)_7$, was selected. The Mean Average Percentage Error (MAPE) for this model was 7.81%. After selection, an investigation of its performance was made using a cross-validation through a rolling window analysis, forecasting up to 30 days ahead (testing period of one year). The results showed that error do not exceed a MAPE of 20%. This allows taking better resource managing decisions in real scenarios: reactive staff hiring is avoided given the reduction of uncertainty for the medium term forecast, which translates into lower costs. Finally, a methodology for the selection of forecasting models is proposed, which includes other constraints from resource management, as well as the different impacts for social well-being.

1. Introduction

The diseases related to respiratory problems belong to the top ten group of the most frequent in the world (Forum of

* Corresponding author.
E-mail address: alejandro.jerez@alumnos.usm.cl (A. Jerez).

https://doi.org/10.1016/j.scitotenv.2019.134978
0048-9697/

International Respiratory Societies (FIRS), 2017). Some of the most relevant illness are the flu, asthma and the common cold, having a short term period (*e.g.* cold lasts 3–7 days). If any of them are not correctly treated, they could derive in a severe case. An example of the previous is pneumonia, which is the main cause of death of children under 5 years old (World Health Organization, 2013).

The main issues of large cities are related to environmental pollution, overcrowding and traffic jams (Villalobos et al., 2013; Wong et al., 2019). The first has great impact on human life (Ma et al., 2018; Torres et al., 2018). The presence of the particulate matter (PM 2.5 and PM10) in the atmosphere results in negative effects on the population (respiratory system): allergies, asthma and oxidative stress (Li et al., 2016; Chen et al., 2016). Additionally, the exposure to contaminants such as Nitrogen Oxides (NO_x) and Sulfur Oxides (SO_x) increases the frequency and severity of diseases (Schlatter, 1994). In particular, extended exposure impacts permanently on life quality, being deadly if the concentration of contaminants passes a certain threshold. The previous is more relevant for elderly and youth (Landrigan et al., 2019; Chen et al., 2019; Boezen et al., 2005).

The capital of Chile, Santiago, is an excellent case for studying the impact of unhealthy air quality. The population is approximately 5.2 million (Instituto Nacional de Estadística (INE), 2017) and the city has geographic conditions that prevent adequate ventilation (Ragsdale et al., 2013). This last factor is relevant, as poor air quality conditions are sustained for up to 5 days (Mazzeo et al., 2018). This triggers the activation of many protocols already determined by the authorities, called "Plan de Descontaminación Atmosférica" (Plan of Atmosphere Decontamination). For instance, sports activities are suspended in schools, vehicular constraints are forced and combustion heating system in industries and housing are forbidden (Ministerio del Medio Ambiente (MMA), 2019).

From the Health Service perspective, the current Social Security system in Chile allows to select an affiliation to the government program FONASA (Fondo Nacional de Salud, National Health Fund), or join the private option called Isapre (Instituciones de Salud Previsional, Health Provision Institutions). The second alternative requires a higher level of income (Rotarou and Sakellariou, 2017). Also, significant differences exist between these systems, both in coverage, cost and quality of service: waiting time, listed diseases, specialization of medical doctors, among others (Dintrans, 2018).

The public health service shows capacity problems when high user demand appears, especially in the Emergency Service. For example, patients have to wait several hours to get medical assistance. Also, medical staff work long shifts, having insufficient infrastructure, and out-of-date equipment (Goic, 2015).

The most critical period is winter, due to the increase of respiratory diseases given the environment pollution of Santiago (Franck et al., 2015). Therefore, the Hospital Administration needs to manage properly the staff requirement (*e.g.* winter vaccination campaigns), medical supplies and stretchers (Carvalho-Silva et al., 2018). Furthermore, given the fact that 30–40% of the total admissions of the Emergency Service presents respiratory causes (Departamento de Estadisticas e Información de Salud, 2019), the possibility of forecasting would become an useful tool. This allows the peaks of the season to be mitigated, and to absorb the inherent variability of users.

This topic is not novel in the literature. Several researchers have worked in performing hospital admission forecasting for different diseases. Generalized Autoregressive Moving Average (GARMA) models have been used to forecast weekly counts of patients with influenza at Hopkins Hospital Emergency Department in Baltimore (Jalalpour et al., 2015). Carvalho-Silva et al. (2018) performed a comparison between Autoregressive Integrated Moving Average (ARIMA) and Exponential Smoothing forecasting models for patients's arrivals at the Emergency Department, up to a week ahead in Braga Hospital, Portugal. ARIMA models have been compared to Artificial Intelligence approaches, such as: Artificial Neural Network (ANN), Random Forest (RF) and Gradient Boosting Machines (GBM), in order to forecast daily hospital admissions due to respiratory causes, across the region of Madrid (Navares et al., 2018). Also, Whitt and Zhang tested a Seasonal ARIMA with exogenous regressors (SARIMAX), such as temperature and calendar variables (holidays), to forecast daily arrivals and hourly occupancy at Rambam Hospital in Haifa, Israel (Whitt and Zhang, 2019).

Currently, the approaches evaluate the predictive capacity of the models for short term forecast: one day or week ahead at the most. This restricts resource management, making it difficult to take an optimal decision for medium term (weeks and months). Also, the use of exogenous variables requires the prior development of an independent procedure to forecast them, as well as a reliable source of information that provides them.

Therefore, this research aims to identify a reliable modelling approach for forecasting the respiratory emergency admissions in the medium term. This would allow cost to be reduced and support to be given to other initiatives, as well to respond better to society's demand in the season peak.

This work is organized as follows: Section 2 presents a description of the geographic area and the data collection used in this study. Section 3 establishes the methodology and data processing. In Section 4, the results and performance analysis are exhibited. The discussions are addressed in Section 5, where recommendations to improve the current approaches are made. Fig. 1 summarizes this standard linear approach for forecasting research. Finally, Section 6 presents the main conclusions of the work and future research guidelines are suggested.

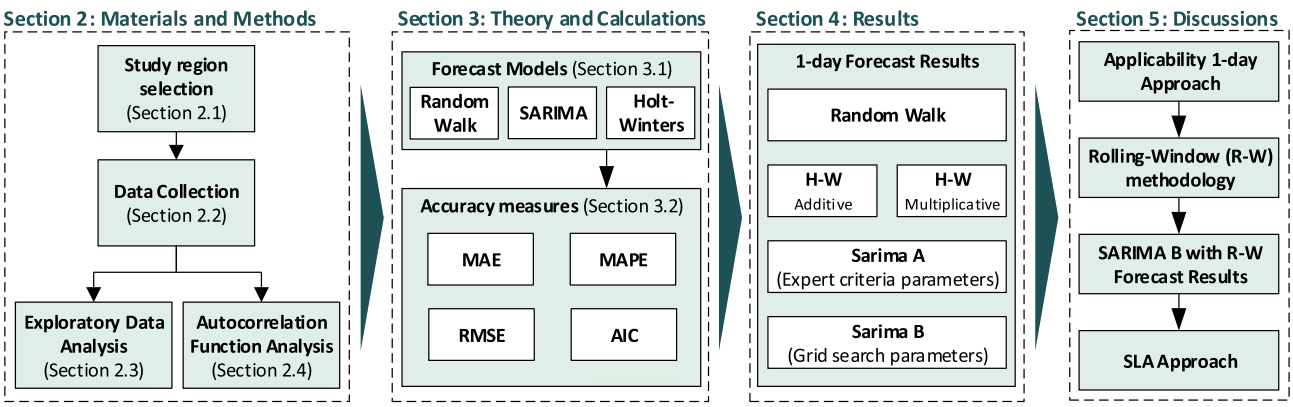

Fig. 1. Summary of the methodology/structure for the present investigation.

2. Materials and methods

2.1. Study region

The geographical area of study is the Metropolitan Region of Santiago, capital of Chile, located 600 meters above sea level, approximately 100 km from the Pacific Ocean coast and 50 km from the border with Argentina. Santiago represents approximately 30% of the population of country (Instituto Nacional de Estadística (INE), 2017). According to the climatic classification of Köppen-Geiger, Santiago has a Bsk climate (Cold semi-arid), with elements of Csb (warm-summer Mediterranean). The above implies hot and dry summers between November and March, and cold and humid winters between June and August. During 2017, there was an average temperature of 22 °C in summer, 9 °C in winter and 278 mm of rain precipitation (Dirección Metereológica de Chile (METEOCHILE), 2017).

Furthermore, Santiago's Emergency Service is composed by a network of 18 high complexity hospitals and 89 SAPUs (Servicio de Atención Primaria de Urgencia, Primary Emergency Attention Service). SAPU treats lower complexity cases and provides first aid. Finally, Fig. 2 shows the exact location of Santiago and the geographical distribution of both facilities addressed before.

2.2. Data collection

The information used in this study was obtained from DEIS (Departamento de Estadística e Información de Salud, Department of Health Statics and Information), which is part of MINSAL (Health Ministry) (Departamento de Estadisticas e Información de Salud, 2019). To be more precise, the platform named "Estadísticas de Atenciones de Urgencia", where only the public admissions are recorded, was the source of data. It is important to remark that this platform filters the record, curing and eliminating voids in the information. Other authors have used this repository for research. An example is Franck et al. (2015, 2014): they studied the admissions related to respiratory and cardiovascular diseases.

Fig. 3 shows a scheme of the data collection for the DEIS database. The admission of a sick patient triggers the process. After been attended a record of the diagnosis is classified following ICD-10 guidelines (World Health Organization, 2016). The information is saved locally, for uploading and recording in a server. Afterwards, through the previously referred to online platform, public access is available, showed with daily resolution and updated everyday.

For the present work, only respiratory diseases were considered. Table 1 contains a full description of them. It is important to clarify that from this point onward, the reference to a time series will mean the aggregated emergency admissions, not being exclusively of a single disease or a group of them.

2.3. Exploratory data analysis

Before modelling the emergency admissions in the time domain, it is important to understand how it behaves. An usual approach is the Exploratory Data Analysis (EDA). This process is

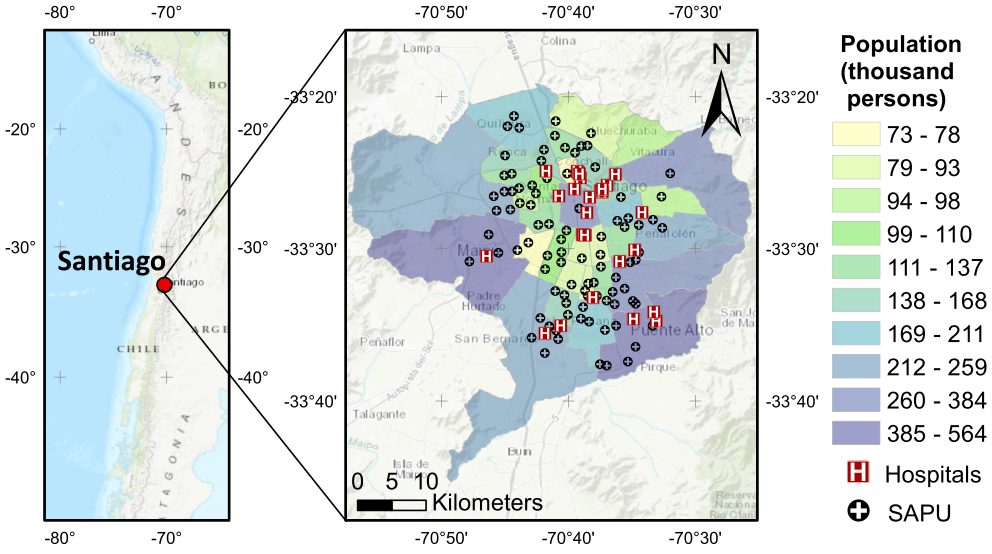

Fig. 2. Map of Metropolitan region of Santiago, Chile.

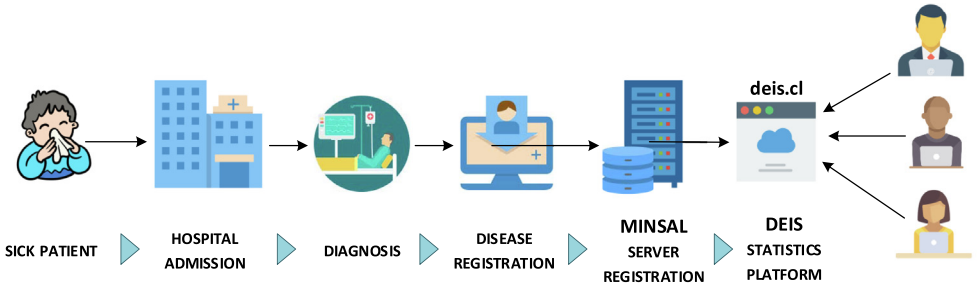

Fig. 3. Step by step process for data collection (DEIS database).

focused on the graphic representation of the data (Tukey, 1977), in order to extract and interpret cyclic behaviors. These descriptions facilitate the selection of models, and they help to avoid misleading patterns.

Fig. 4 shows the hospital admissions and PM 2.5 time series. An annual periodicity is observed in these series, with higher values (peaks) in the autumn–winter months. On the other hand, spring-summer months have less variability and lower values. In particular, Franck et al. found significant effects on respiratory hospital admissions because the presence of particular matter (Franck et al., 2015).

Nevertheless, several factors can also explain this behavior. For example, Elshorbany et al. and Rasgsdale et al. addressed this phenomena as result of the poor ventilation of Santiago (Elshorbany et al., 2010; Ragsdale et al., 2013). Descriptive statistics of the aggregated series of emergency hospital admissions due to respiratory diseases is summarized in Table 2.

Table 1
Database classification by group of respiratory disease, according to ICD-10 coding.

ICD-10	Disease
J00-J06	Acute upper respiratory infections
J09-J11	Influenza
J12-J18	Pneumonia
J20-J21	Acute Bronchitis/Bronchiolitis
J40-J46	Chronic Obstructive Pulmonary, Chronic Bronchitis, Emphysema and Asthma
J22, J30-39, J47, J60-98	Unspecified acute lower respiratory infection, other diseases of upper respiratory tract, bronchiectasis, lung diseases due to external agents and others

When analyzing the number of emergency admissions according to the day of the week, the second part of week (from Thursday to Saturday) concentrates the activity, having a peak on Saturday. This day has the particularity of presenting the greatest variability as well, in other words, the difference between its extremes values. On the other hand, Wednesday has the lowest activity, as well as the lowest variability (see Fig. 5). This may suggest a behavior of

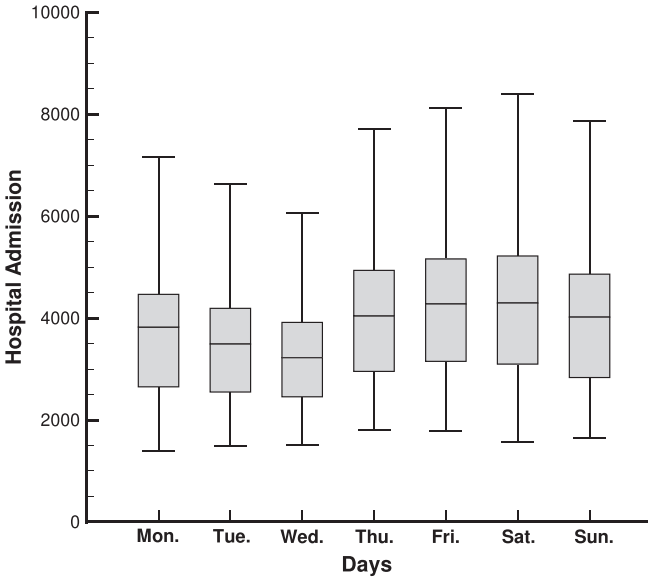

Fig. 5. Boxplot of emergency admissions per day of the week for period 2014 to 2018.

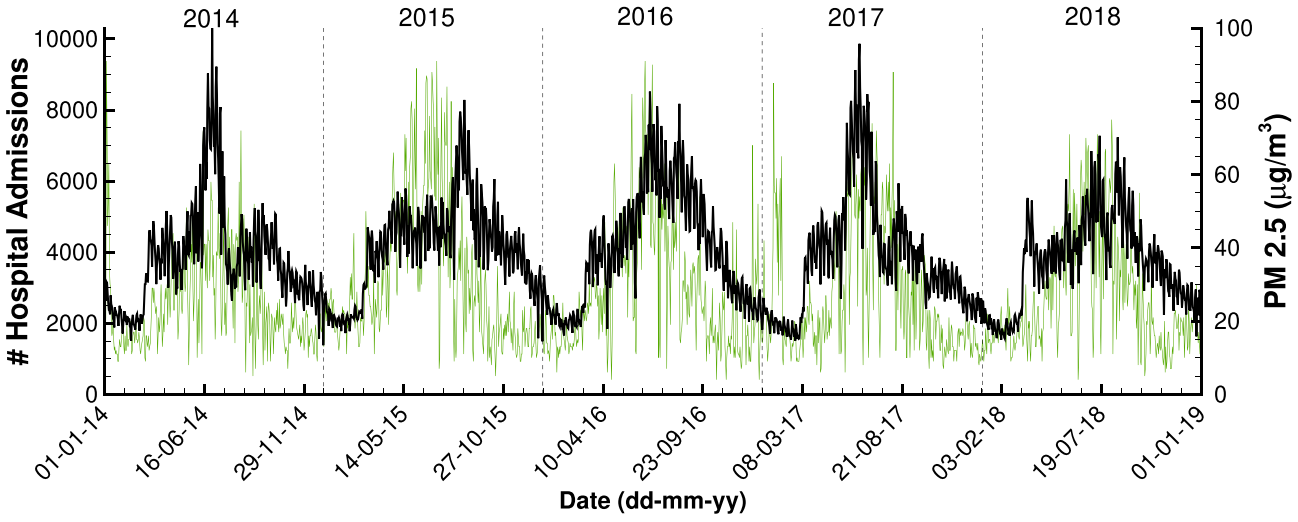

Fig. 4. Total emergency admissions (black) and PM 2.5 (green) time series, which comprehended 5 years of data.

Table 2
Summary statistics for the emergency admissions due respiratory diseases time series.

Mean	Median	Max	Min	St. Dev.	Skewness	Kurtosis
3,912	3,818	10,305	1,383	1,475	0.757	3.589

delaying the visit to Emergency Services, which is saturated during weekends (more than 4,000 average attentions every day).

2.4. Autocorrelation function

The sample autocorrelation function (ACF) and partial autocorrelation function (PACF) are useful in the identification of periodic patterns and dependence structures (Hamilton and Watts, 1978). The graphical representation of these functions provides additional information about the variations of the emergency admissions time series, and can be used to perform feature selection procedures too. Fig. 6 represents the sample ACF and PACF for the first 60 lags. Let y_t be the value of the time series at time t and $\bar{y}$ its mean, the lag k autocorrelation coefficient, r_k, measures the linear correlation of the time series at times t and $t-k$, and it is given by:

$$r_k = r(y_t, y_{t-k}) = \frac{\sum_{t=k+1}^{n} (y_t - \bar{y})(y_{t-k} - \bar{y})}{\sum_{t=1}^{n} (y_t - \bar{y})^2} \quad (1)$$

Where n is the length of the observed series. Moreover, PACF measures the degree of direct correlation between two observations, y_t and y_{t-k}, when the effects of periods other than k are isolated from the analysis.

As can be seen in Fig. 6a, autocorrelation for close lags is large and positive, in terms of time and magnitude. The above feature is usual in time series with a predominant trend. Moreover, the autocorrelations reveal a seasonal behavior with high values for intervals of one week and their multiples (7 days) in comparison with the rest of the week.

The ACF tails off slowly as the lags increase due to the trend, while the bumps appear due to weekly seasonality. From the PACF presented in Fig. 6b, it is possible to confirm the systematic seasonality indicated by the analysis of ACF for the periodic pattern of 7 days. The aforementioned suggests the presence of autoregressions in the process for lags present up to 7 days ago.

In conclusion, the graphic analysis suggests the presence of seasonality and autocorrelation in the time series. Then, it is appropriate to propose forecast models that incorporate these effects. In Section 3.1, different forecast models that incorporate this weekly cycle will be revised.

3. Theory and calculations

In this section, different models are investigated for the emergency admissions time series. These models have different levels of complexity, which makes the trade-off evaluation in the selection of the optimal model relevant. This evaluation will be in terms of the interpretation and the computational cost to solve it.

3.1. Models

Firstly, the forecast models were calibrated accordingly to the results of the exploratory analysis presented in Section 2.3. Secondly, in order to establish an unbiased selection method, a part of the time series under study was separated to perform the training of the models. This part included the first four years (2014–2017). Then, the testing period is 2018. A graphic explanation is provided in Fig. 7.

As a first approach, it seems plausible to consider a benchmark method that takes into account the seasonality prevailing in the emergency admissions time series. We set the seasonal random walk with weekly seasonality as baseline. Here, the predicted value for the forecast horizon h is considered to be equal to the observed value from previous week, that is: $\hat{y}_{T+h|T} = y_{T+h-m}$, being $m = 7$ the weekly seasonal period. This kind of approach requires no parametrization or setup, and it is often used to establish a benchmark method rather than a model of choice (Hyndman, 2010).

The following step is to select an improved methodology. Box-Jenkins method (Box et al., 2015) has been widely used as an approach to time series modelling and forecasting. In this model, the estimated value of a variable corresponds to a linear combination of the previous values and errors of the series. Thus, the Auto-Regressive terms (AR) and the Moving Averages (MA) constitute two different parts of the approach, which is also called ARMA because of the mentioned elements.

In various situations, a time series can be considered as composed of a non-stationary trend component and a stationary component of zero mean. In this case, it is useful to differentiate such characteristics to obtain a stationary process. The ARIMA, or integrated ARMA, is a type of ARMA model that incorporates a differentiation procedure into the modeling. To further details of this modelling, please refer to Appendix A.

When there is past dependence in multiples of the underlying lag s, it is possible to introduce modifications to the ARIMA model to take into account seasonal and non-stationary behaviors. This approach is called Seasonal Auto-Regressive Integrated Moving Average, and denoted as SARIMA $(p,d,q)(P,D,Q)_s$. This mathematical extension of ARIMA can be found in Appendix A.

SARIMA model parameters can be obtained by optimizing the likelihood function expressed in Eq. A.2. Because of the risk associated with overlooking an optimal model when selecting the hyperparameters p,d,q,P,D,Q,s, it is possible to approach the problem by searching through the space of feasible models, to obtain the best solution in a certain neighborhood. The identification of SARIMA models through the use of a performance metric or information criterion can be automated using a grid search procedure (further discussion can be found in Section 3.2). Moreover, the efforts to accomplish this search can be reduced by taking into account the findings obtained from Section 2.3. This allows to decrease the domain of feasible hyperparameters for SARIMA models. In addition, the degree of the autoregressive polynomials and moving averages is usually not high (Shumway and Stoffer, 2017). Therefore, grid search is an attractive approach solution for this type of problem.

Finally, the seasonal characteristics of the series allows to compare the proposed SARIMA model with the seasonal extension of Holt-Winters (H-W) method (Holt, 2004; Winters, 1960). The mathematical modelling and a brief explanation are presented in Appendix B.

3.2. Accuracy measures

The accuracy of a forecasting model can only be determined by considering how well it performs with data that has not been included in the estimation process. To evaluate a model, the available data is separated in two different sets: training and test. The training data set is used to estimate model parameters and to adjust hyperparameters in a portion of the training set (validation set). This specifies how the training will be carried out for a forecast model. Then, the test data is used to evaluate the accuracy of the training set (Hyndman and Athanasopoulos, 2018; Khaldi et al., 2019).

There is no rule to determine the size of the training and testing sets. However, a general practice is to use 20% of the total data as the test set (Trevor et al., 2009).

To assess the accuracy of the forecast models, generally the used metrics are based on the forecast error $e_t = \hat{y}_t - y_t$, which

considers as error the unpredictable portion of an observation at time t. Although there are many error prediction metrics, there is not one which is universally accepted (Hyndman and Koehler, 2006). The most common performance metrics are the Mean Absolute Error (MAE), Mean Absolute Percentage Error (MAPE) and Mean Squared Error (MSE) (Zivot and Wang, 2007):

$$\mathrm{MAE} = \frac{1}{n}\sum_{t=1}^{n}|\hat{y}_t - y_t| \tag{2}$$

$$\mathrm{MAPE} = 100 \cdot \frac{1}{n}\sum_{t=1}^{n}\left|\frac{\hat{y}_t - y_t}{y_t}\right| \tag{3}$$

$$\mathrm{RMSE} = \sqrt{\frac{1}{n}\sum_{t=1}^{n}(\hat{y}_t - y_t)^2} \tag{4}$$

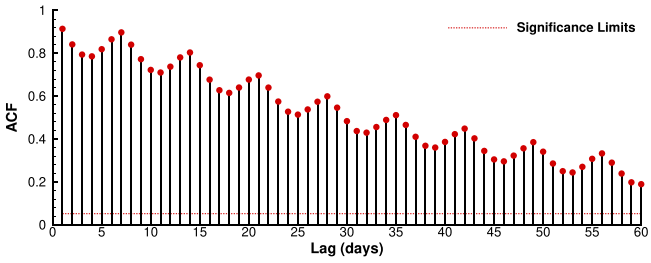

(a) ACF

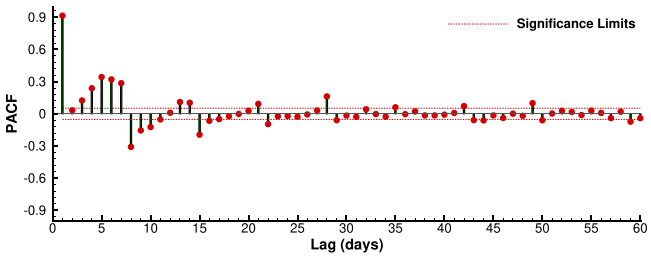

(b) PACF

Fig. 6. Autocorrelation functions for the emergency admissions time series.

Where the period under evaluation has a total of n observations for the estimation process.

Generally, MAPE is used to compare the performance of forecasts through different size sets of data because its scale independence. On the other hand, MAE and RMSE are scale-dependent metrics (useful in same data set). Nevertheless, they are more sensitive to outliers than other metrics, but widely used due to their theoretical relevance in statistical modeling (Hyndman and Koehler, 2006).

If the aim of the model selection is to grant parsimony and penalty to the variance of the error ($\hat{\sigma}_u^2$, where u stands for the number of required parameters), the use of the Akaike information criterion (AIC) is a common choice (Box et al., 2015). The aforementioned means that the best model does not underestimate or overestimate the underlying error.

$$AIC = \log \hat{\sigma}_u^2 + \frac{n + 2u}{n} \tag{5}$$

4. Results

In this section, the results obtained when performing one-day forecasts are presented. Also, a rolling window analysis is shown, considering the observations of the test set (year 2018), as presented previously in Fig. 7. The models implemented were: seasonal random walk, additive and multiplicative Holt Winters, and SARIMA with parameters $(p,d,q)(P,D,Q)_s$. For this last model, two cases were investigated: case A, using parameters defined according to the insights obtained in Section 2.3; and case B, where the parameters were obtained with the best solution from the grid search, using AIC as key performance indicator for each differentiation order. Accuracy measures obtained within the training data for each of the proposed forecasting models are shown in Table 3.

Firstly, it is possible to establish the performance results obtained with the seasonal random walk model as baseline. The MAPE is 12.09%, which implies that any model with less than 12.09% sets an improvement in comparison with this approach.

Holt-Winters models shows a better accuracy performance, decreasing the MAPE by 2% (multiplicative). In terms of RMSE, both approaches (additive and multiplicative) are similar.

Then, the case A in SARIMA modeling was defined with the parameters $(1,1,0)(1,1,0)_7$, which are determined by using the

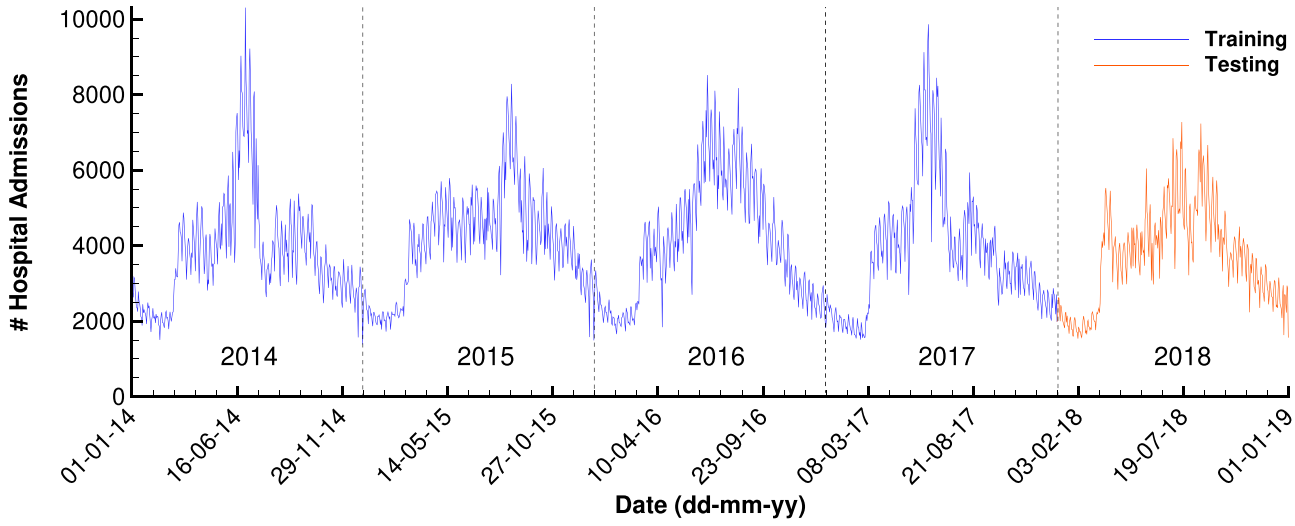

Fig. 7. Total emergency admissions time series with differentiation of Training data (2014–2017) and Testing data (2018).

Box–Jenkins methodology, according to the insights obtained in Section 2.3. This model improves the performance of the error: 1% lower than multiplicative H-W. The case B is defined with the parameters obtained from a grid search. The number of different combinations of parameters is 8,448, according to the domain set presented in Table 4.

From the above, the model with the lowest AIC was selected: $(2,1,3)(3,0,2)_7$. This last model's accuracy presented a MAPE of 7.81%, decreasing the error 1% more. However, it is important to remark that the computational cost associated with decreasing the MAPE by 13% from case A to the parametrization used in the case B, requires a total of 8 h, considering a parallel processing in 16 cores at 2.93 GHz.

Fig. 8 shows the comparison between the forecasting of SARIMA model (case B) and the observed data of the testing period (data 2018). It is clear that the model captures seasonality observed in the time series during the winter season, where the hospital emergency admissions are higher compared to summer due to an increase in environmental pollution (Franck et al., 2015). However, despite the correct behaviour, it has problems related to underestimating extreme values (smoother forecasting than reality).

Table 3
Summary from different modeling approaches

Model	Training Data			
	AIC	MAPE	MAE	RMSE
Random Walk ($t-7$)	-	12.09%	479.45	676.75
H-W Additive	-	10.51%	408.26	585.18
H-W Multiplicative	-	10.05%	403.73	584.19
SARIMA case A	22,408	8.97%	357.23	516.92
SARIMA case B	21,932	7.81%	299.88	436.71

Table 4
Grid search for SARIMA B parameters

Parameter	Domain set
p	{0,1,2,3}
d	{0,1,2}
q	{0,1,2,3}
P	{0,1,2,3}
Q	{0,1,2,3}
S	{0,...,10}

Figs. 9 and 10 show that cold seasons (autumn, winter) are more difficult to forecast than the rest of the year, in other words, the error of this period shows greater volatility. In particular, it is of important to realize that the peak of winter would require a greater capacity of hospital care, compared to the time series of spring and summer. Also, the results suggest that forecasting efforts during the year could focus only on the seasons of high admission levels. For instance, proposing a specific model for each season could improve the accuracy, but this is out of the scope of the present work.

5. Discussions

The forecast results presented in the previous section only estimate one-step ahead predictions. Unfortunately, this approach does not provide a sufficient time span to make any realistic decision in response to demand variations and may not be as relevant as multi-step forecasts. Thus, using this model as a tool for managing hospital resources at medium and long term is inadequate. Therefore, an important improvement to the model must consider the capability of estimating a horizon that allows management decisions such as: hiring of transitory services (Gerardo et al., 2018), reinforcement of worker shifts, more medical staff, among others. Then, testing the capabilities of SARIMA model at different time horizons m is needed. For this task, it is possible to evaluate the predictive performance of the forecasting model using a rolling window of m consecutive observations. The previous formulation is displayed schematically in Fig. 11, and may have different approaches. For example, the training set can always start at the first sample and be expanded in time, hence, the training set size will vary over the time splits. On the other hand, a fixed window approach moves the training set while keeping the training set size fixed over time.

For the respiratory emergency admissions series we applied this time series cross-validation scheme, performing multi-step forecasts ($h = 1,\ldots,30$) with model parameter re-estimation for each fixed window, as shown in Fig. 12 for $h = 7$. In addition, SARIMA model hyperparameters for case B were selected to run the modeling (for further details, see Section 4). Later, the estimators of the model are re-calculated in each forecast process with new data training set.

The calculated MAPE for each rolling window horizon is equivalent to the average of the corresponding prediction (see Fig. 13). It

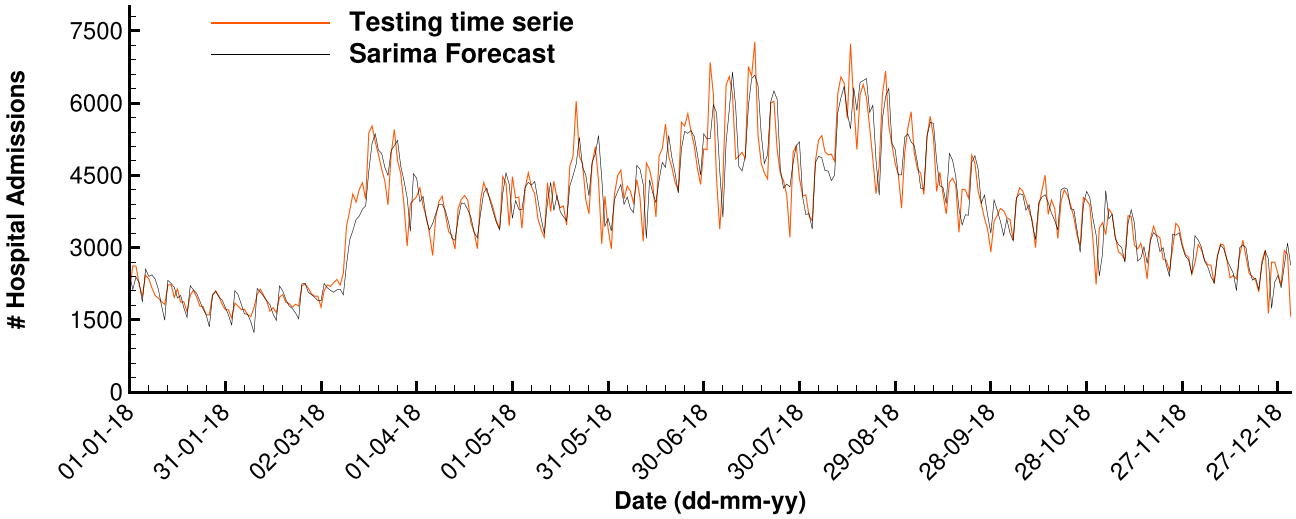

Fig. 8. Forecast results for SARIMA modeling, case B.

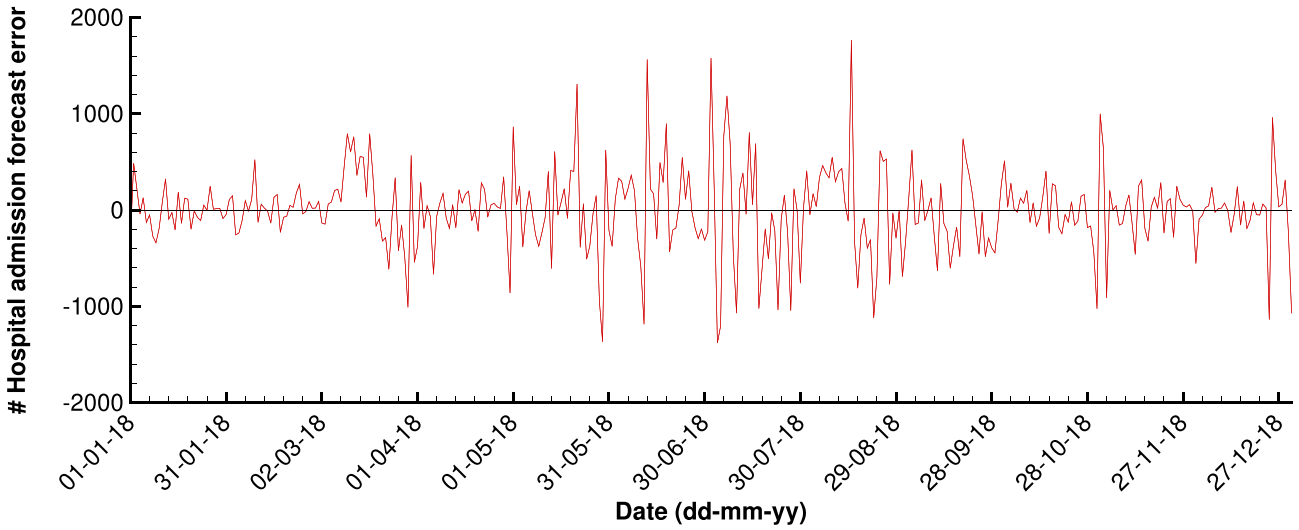

Fig. 9. Forecast error in testing period.

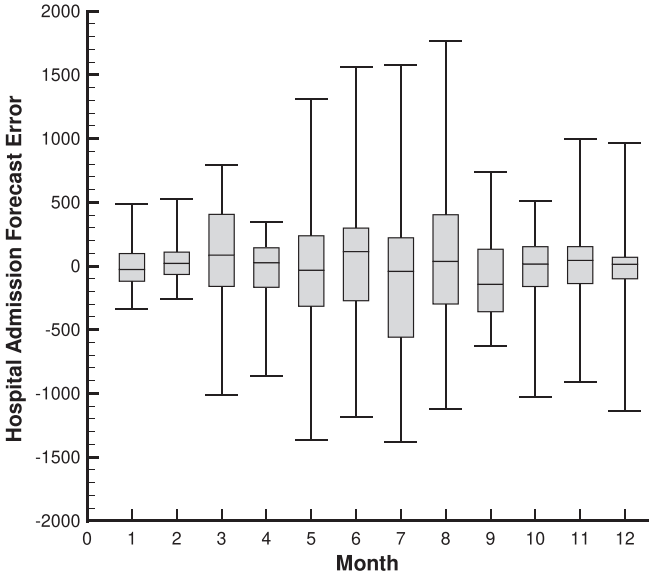

Fig. 10. Forecast error boxplot, monthly aggregated. January corresponds to 1 and December to 12.

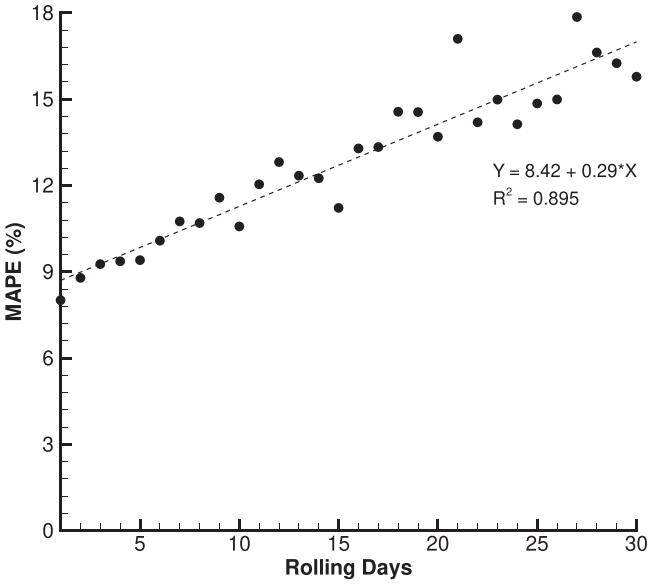

Fig. 13. MAPE evolution in function of rolling window horizon.

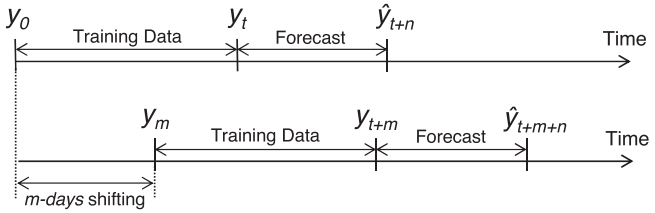

Fig. 11. Different validation approaches through a rolling window.

is important to clarify that due to the nature of this exercise, the width of horizon window is inversely proportional to the number of simulations that can be performed. However, this difference of MAPEs for each window is neutralized by the fact that the MAPE of the widest window incorporates the error of a higher number of days.

As expected, as the forecast horizon increases the error of the estimation for the emergency admissions generally increases. The explanation for this is the propagation of the error across the

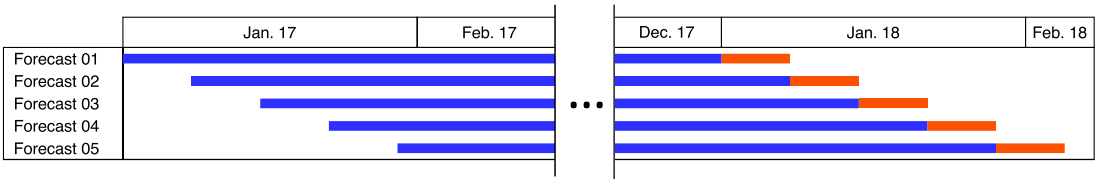

Fig. 12. Rolling window application methodology with a 7-day horizon. Blue bar represents Traninig Data and orange bar is the Forecast.

forecast window. The most accurate of the rolling windows shows an error of 8%, which is achieved with one-day's size. If a simple regression is performed, the error when estimating one month in advance should not exceed 20% in any case (see Fig. 13).

Because of the nature of the addressed problem, an important dimension to discuss is to quantify the population involved within the estimation of errors. A suitable indicator is the MAE, considering a slight modification: only the underestimation of emergency admissions should be weighed. For example, if a 30-day horizon rolling window had been used (which contains the greatest MAPE), a total of ~750,000 people would be over/underestimated. However, given that an overestimation of the forecast does not affect any person, the error decreases to ~200,000 people annually.

There are many applications for the forecast of emergency admissions. A simple example is to improve the strategy of hiring professionals, in order to meet the changes in health care demand. In this way, if the health institution manages its budget better by optimizing its headcount, it could redirect the resources to other priority activities. In Chile, within the professionals with permanent contracts, there are two ways to enroll professional staff to respond to the peak of demand and seasonal variation:

- Fixed term employees: professionals hired directly by the hospital and/or health centre, whose contract is for a fixed term of days (usually around 30 days).
- Transitory services: corresponds to professionals who attend sporadically to provide support to the institution, hired by an external agency, which provides these type services to the health institution. In Chile, the use of this kind of services is regulated for the law 20,123 and can not be used permanently (Gerardo et al., 2018; Congreso Nacional de Chile, 2007).

It is important to identify, at least qualitatively, that the unit cost per working hour is not equal in each scheme. A fixed term employee has a lower cost than a transitory service one. Therefore, a well managed institution, which is able to forecast accurately the users, should distribute its total cost for each scheme efficiently: fixed term employees to face medium term demand peaks (*e.g.* winter or monthly increases), while transitory services are only hired to meet the peak of short term demand (*e.g.*: weekly or daily).

Under this scenario, forecasting a few days ahead does not provide the necessary information to implement an efficient strategy to react to the demand variation. In particular, a forecast with a horizon of 2 weeks or more would probably allow decisions to be taken and the necessary arrangements made. Then, any forecast smaller than this horizon would only allow to choose the option of transitory services, with the corresponding higher cost. In order to have enough information to balance between fixed term employees and transitory services, the size of the forecast horizon must be one month (4 weeks).

The execution of a competent resource management in any health institution that implements a 4-week horizon forecasting, requires an adequate indicator to evaluate the performance of the model. From a social perspective, the existing cost of not having the capacity to provide health care to emergency admissions is greater than having an unemployed capacity, for which a revised version of the MAE (MAE_R) is presented in Eq. 6.

$$MAE_R = \frac{1}{n}\sum_{t=1}^{n}|\hat{y}_t - y_t| \cdot \omega_t \tag{6}$$

Here, ω_t stands for a piecewise function that penalizes the absolute error given the type of forecast error in the evaluation in time t, according to a range of Service Level Agreements (SLAs). Different scenarios presented in Fig. 14 (with arbitrary SLA levels), where three situations can happen:

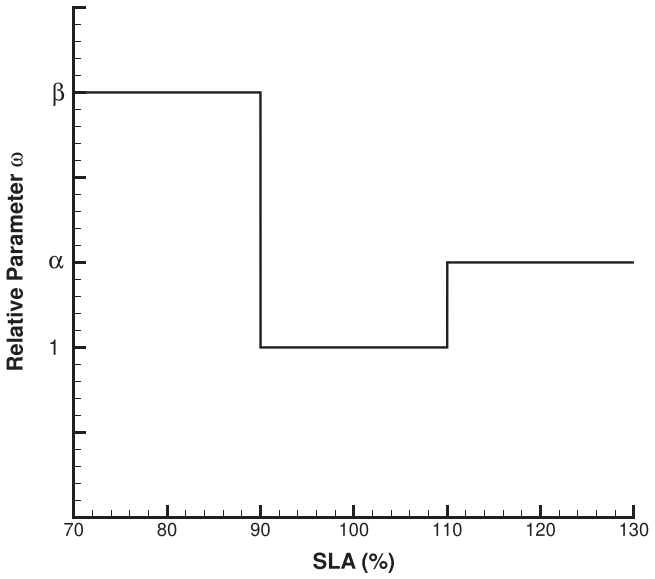

Fig. 14. Piecewise function for penalty parameter ω_t.

- SLA less than 90%: an error escalation is applied by parameter β.
- SLA higher than 110%: an error escalation is applied by parameter α, such that $\alpha < \beta$. This applies a greater penalty to the underestimation of the demand than to the overestimation.
- SLA between 90–110% (included): not apply penalty to forecast error ($\omega = 1$), because it is within a permissible range that is capable of controlling the emergency service.

The guarantee of a SLA is essential in an emergency admissions context, where people's lives are at risk. Also, a larger staff headcount ensures that the above mentioned is fulfilled. Being able to justify the level of penalty for the parameter ω in the metric, as well as specify how the parameters affect the indicator (values of β and α), are subject for another extended study. For example, a linear piecewise function has been presented illustratively in the present work, however, it may have a smooth behavior as logarithmic or exponential functions.

6. Conclusions

An accurate forecasting of emergency admissions due to respiratory diseases is relevant in the context of managing the resources in a hospital. This allows managers to maximize the utilization of the budget and to avoid inadequate sourcing strategies in high demand seasons.

For the particular case of Santiago de Chile, the collected data suggest a SARIMA modelling. The error differences obtained between Box–Jenkins methodology and a complete grid search is around 1% (MAPE). The hyperparameters of the best model were with parameters $(p,d,q)(P,D,Q)_S = (2,1,3)(3,0,2)_7$, showing a MAPE of 7.81%.

In order to reduce the uncertainty level, aiming to take better decisions, the forecast horizon must be expanded considerably. From the perspective of the authors, at least 15 days ahead is the minimum for actual deployment of decisions. The sensibility analysis of rolling window shows that the MAPE for that period is around 13%. In the case of 30-day forecast, the error should be not greater than 20%.

Furthermore, when using the forecast model presented, the manager should consider using a metric to take into account the social cost involved when providing a certain service level agree-

ment to the community, and how much budget is allowed to be spent providing it.

Finally, future work should aim to improve the management of outliers and holidays for the time series. Also, selecting a model for each season could provide a deeper insight of the phenomena (winter especially). Another perspective should be trying to use exogenous variables for the forecast (multivariable forecasting), such as the temperature, humidity and others.

Declaration of competing interest

The authors declare that they have no known competing financial interests or personal relationships that could have appeared to influence the work reported in this paper.

Acknowledgments

The authors recognize the valuable support from BHP Chile Inc. regarding the English review of the article. Bastián Aballay thanks the partially support from DGIP, UTFSM, Chile; through the PIIC initiative. Hugo O. Garcés thanks support from CORFO-Chile under Grant 18iip-bb-99513. Finally, authors thank to DEIS-MINSAL for available information on the online platform of hospital emergency admissions.

Appendix A: ARIMA and SARIMA models

ARIMA modelling can be expressed as follows:

$$\phi(B)(1-B)^d y_t = \theta(B)\varepsilon_t \tag{A.1}$$

Where y_t is the observed time series (as mentioned in previous sections), and ε_t is a white noise Gaussian process. Autoregressive and moving average components are represented by the operators $\phi(B) = 1 - \phi_1 B - \phi_2 B^2 - \ldots - \phi_p B^p$ and $\theta(B) = 1 + \theta_1 B + \theta_2 B^2 + \ldots + \theta_q B^q$ for polynomials with order p y q, respectively. Here, the differencing operator of order d is denoted by $(1-B)^d$ and $Bx_t = x_{t-1}$ is the time series backshift operator.

SARIMA $(p,d,q)(P,D,Q)_s$ extends the ARIMA model described above, through this equation:

$$\Phi_P(B^s)\phi(B)\nabla_s^D\nabla^d y_t = delta + \Theta_Q(B^s)\theta(B)\varepsilon_t \tag{A.2}$$

Here, the autoregressive components and seasonal moving averages are denoted by $\Phi_P(B^s)$ and $\Theta_Q(B^s)$ of order P y Q, respectively. The ordinary differencing operator of order d is denoted by $\nabla^d = (1-B)^d$ and the seasonal difference component is given by $\nabla_s^D = (1-B^s)^D$.

Appendix B: Winter-Holts

This method includes the use of one forecast equation and three smoothing equations: the level l_t, the trend b_t and the seasonality s_t. These smoothing parameters are α, β and γ, respectively. Depending on the seasonal nature of the series, the specification could be additive, when seasonal variation is approximately constant throughout the series; or multiplicative, when the seasonal component changes with the level of the series. Let m be the frequency of seasonality and v the integer part of $(h-1)/m$, both methods can be expressed as follows:

$$\begin{aligned}\hat{y}_{t+h|t} &= l_t + hb_t + s_{t+h-m(v+1)} \\ l_t &= \alpha(y_t - s_{t-m}) + (1-\alpha)(l_{t-1} + b_{t-1}) \\ b_t &= \beta(l_t - l_{t-1}) + (1-\beta)b_{t-1} \\ s_t &= \gamma(y_t - l_{t-1} - b_{t-1}) + (1-\gamma)s_{t-m}\end{aligned} \tag{B.1}$$

$$\begin{aligned}\hat{y}_{t+h|t} &= (l_t + hb_t)s_{t+h-m(v+1)} \\ l_t &= \alpha\frac{y_t}{s_{t-m}} + (1-\alpha)(l_{t-1} + b_{t-1}) \\ b_t &= \beta(l_t - l_{t-1}) + (1-\beta)b_{t-1} \\ s_t &= \gamma\frac{y_t}{l_{t-1}+b_{t-1}} + (1-\gamma)s_{t-m}\end{aligned} \tag{B.2}$$

References

Boezen, H., Vonk, J., Van der Zee, S., Gerritsen, J., Hoek, G., Brunekreef, B., Schouten, J., Postma, D., 2005. Susceptibility to air pollution in elderly males and females. Eur. Respir. J. 25 (6), 1018–1024. https://doi.org/10.1183/09031936.05.00076104.

Box, G.E., Jenkins, G.M., Reinsel, G.C., Ljung, G.M., 2015. Time series analysis: forecasting and control. John Wiley & Sons.

Carvalho-Silva, M., Monteiro, M.T.T., de Sá-Soares, F., Dória-Nóbrega, S., 2018. Assessment of forecasting models for patients arrival at emergency department. Operations Res. Health Care 18, 112–118. https://doi.org/10.1016/j.orhc.2017.05.001.

Chen, R., Hu, B., Liu, Y., Xu, J., Yang, G., Xu, D., Chen, C., 2016. Beyond pm2. 5: the role of ultrafine particles on adverse health effects of air pollution. Biochimica et Biophysica Acta (BBA)-General Subjects 1860 (12), 2844–2855. https://doi.org/10.1016/j.bbagen.2016.03.019.

Chen, Z., Cui, L., Cui, X., Li, X., Yu, K., Yue, K., Dai, Z., Zhou, J., Jia, G., Zhang, J., 2019. The association between high ambient air pollution exposure and respiratory health of young children: a cross sectional study in Jinan, China. Sci. Total Environ. https://doi.org/10.1016/j.scitotenv.2018.11.368.

Congreso Nacional de Chile, LEY NUM. 20.123, Tech. rep., Biblioteca del Congreso Nacional (BNC), http://bcn.cl/1uvqz [Accessed: 2019/06/23] (2007).

Departamento de Estadisticas e Información de Salud, Estadísticas de Atenciones de Urgencia, Tech. rep., Ministerio de Salud, Gobierno de Chile, http://www.deis.cl/estadisticas-atencionesurgencia/ [Accessed: 2019/01/14] (2018).

Dintrans, P.V., 2018. Out-of-pocket health expenditure differences in chile: Insurance performance or selection?. Health Policy 122 (2), 184–191. https://doi.org/10.1016/j.healthpol.2017.11.007.

Dirección Metereológica de Chile (METEOCHILE), Anuario metereológico 2017, Tech. rep., Dirección General de Aeronáutica Civil, https://climatologia.meteochile.gob.cl/application/publicaciones/anuario/2017 [Accessed: 2019/03/18] (2018).

Elshorbany, Y.F., Kleffmann, J., Kurtenbach, R., Lissi, E., Rubio, M., Villena, G., Gramsch, E., Rickard, A., Pilling, M., Wiesen, P., 2010. Seasonal dependence of the oxidation capacity of the city of santiago de chile. Atmos. Environ. 44 (40), 5383–5394. https://doi.org/10.1016/j.atmosenv.2009.08.036.

Forum of International Respiratory Societies (FIRS), The Global Impact of Respiratory Disease, Tech. rep., European Respiratory Society (2017).

Franck, U., Leitte, A.M., Suppan, P., 2014. Multiple exposures to airborne pollutants and hospital admissions due to diseases of the circulatory system in Santiago de Chile. Sci. Total Environ. 468, 746–756. https://doi.org/10.1016/j.scitotenv.2013.08.088.

Franck, U., Leitte, A.M., Suppan, P., 2015. Multifactorial airborne exposures and respiratory hospital admissions-The example of Santiago de Chile. Sci. Total Environ. 502, 114–121. https://doi.org/10.1016/j.scitotenv.2014.08.093.

Gerardo Otero, A., Maria Dolores Echeverria, F., Macarena López, M., María de los Ángeles Fernández, S., 2018. Labour and Employment Compliance in Chile. Wolters Kluwer.

Goic, A., 2015. El Sistema de Salud de Chile: una tarea pendiente. Revista Médica de Chile 143, 774–786. https://doi.org/10.4067/S0034-98872015000600011.

Hamilton, D.C., Watts, D.G., 1978. Interpreting partial autocorrelation functions of seasonal time series models. Biometrika 65 (1), 135–140. https://doi.org/10.1093/biomet/65.1.135.

Holt, C.C., 2004. Forecasting seasonals and trends by exponentially weighted moving averages. Int. J. Forecasting 20 (1), 5–10. https://doi.org/10.1016/j.ijforecast.2003.09.015.

Hyndman, Rob J., 2010. Benchmarks for forecasting, https://robjhyndman.com/hyndsight/benchmarks/ [Accessed: 2019/03/18].

Hyndman, R.J., Athanasopoulos, G., 2018. Forecasting: principles and practice, OTexts.

Hyndman, R.J., Koehler, A.B., 2006. Another look at measures of forecast accuracy. Int. J. Forecasting 22 (4), 679–688. https://doi.org/10.1016/j.ijforecast.2006.03.001.

Instituto Nacional de Estadística (INE), CENSO de Población y Vivienda 2017, http://www.censo2017.cl/ [Accessed: 2019/05/15] (2017).

Jalalpour, M., Gel, Y., Levin, S., 2015. Forecasting demand for health services: development of a publicly available toolbox. Operations Res. Health Care 5, 1–9. https://doi.org/10.1016/j.orhc.2015.03.001.

Khaldi, R., El Afia, A., Chiheb, R., 2019. Forecasting of weekly patient visits to emergency department: real case study. Procedia Computer Sci. 148, 532–541. https://doi.org/10.1016/j.procs.2019.01.026.

Landrigan, P.J., Fuller, R., Fisher, S., Suk, W.A., Sly, P., Chiles, T.C., Bose-O'Reilly, S., 2019. Pollution and children's health. Sci. Total Environ. 650, 2389–2394. https://doi.org/10.1016/j.scitotenv.2018.09.375.

Li, N., Georas, S., Alexis, N., Fritz, P., Xia, T., Williams, M.A., Horner, E., Nel, A., 2016. A work group report on ultrafine particles (aaaai) why ambient ultrafine and engineered nanoparticles should receive special attention for possible adverse

health outcomes in humans. J. Allergy Clinical Immunol. 138 (2), 386. https://doi.org/10.1016/j.jaci.2016.02.023.
Ma, Y., Yang, S., Zhou, J., Yu, Z., Zhou, J., 2018. Effect of ambient air pollution on emergency room admissions for respiratory diseases in Beijing. China, At. Environ. 191, 320–327. https://doi.org/10.1016/j.atmosenv.2018.08.027.
Mazzeo, A., Huneeus, N., Ordoñez, C., Orfanoz-Cheuquelaf, A., Menut, L., Mailler, S., Valari, M., van der Gon, H.D., Gallardo, L., Muñoz, R., et al., 2018. Impact of residential combustion and transport emissions on air pollution in Santiago during winter. Atmos. Environ. 190, 195–208. https://doi.org/10.1016/j.atmosenv.2018.06.043.
Ministerio del Medio Ambiente (MMA), Planes de Descontaminación Atmosférica, Estrategia 2014–2018 - Región metropolitana de Santiago, Chile, Tech. rep., Gobierno de Chile, http://portal.mma.gob.cl/planes-de-descontaminacion-atmosferica-estrategia-2014-2018/ [Accessed: 2019/03/18] (2018).
Navares, R., Díaz, J., Linares, C., Aznarte, J.L., 2018. Comparing arima and computational intelligence methods to forecast daily hospital admissions due to circulatory and respiratory causes in madrid. Stochastic Environ. Res. Risk Assess. 32 (10), 2849–2859. https://doi.org/10.1007/s00477-018-1519-z.
Ragsdale, K.M., Barrett, B.S., Testino, A.P., 2013. Variability of particulate matter (PM10) in Santiago, Chile by phase of the Madden–Julian Oscillation (MJO). At. Environ. 81, 304–310. https://doi.org/10.1016/j.atmosenv.2013.09.011.
Rotarou, E.S., Sakellariou, D., 2017. Neoliberal reforms in health systems and the construction of long-lasting inequalities in health care: A case study from chile. Health Policy 121 (5), 495–503. https://doi.org/10.1016/j.healthpol.2017.03.005.
Schlatter, C., 1994. Environmental pollution and human health. Sci. Total Environ. 143 (1), 93–101. https://doi.org/10.1016/0048-9697(94)90535-5.
Shumway, R.H., Stoffer, D.S., 2017. Time Series Analysis and its Applications: With R Examples. Springer.
Torres, P., Ferreira, J., Monteiro, A., Costa, S., Pereira, M.C., Madureira, J., Mendes, A., Teixeira, J.P., 2018. Air pollution: a public health approach for portugal. Sci. Total Environ. 643, 1041–1053. https://doi.org/10.1016/j.scitotenv.2018.06.281.
Trevor, H., Robert, T., JH, J., 2009. The elements of statistical learning: data mining, inference, and prediction..
Tukey, J.W., 1977. Exploratory Data Analysis, Vol. 2. Reading, Mass.
Villalobos, A.M., Barraza, F., Jorquera, H., Schauer, J.J., 2013. Chemical speciation and source apportionment of fine particulate matter in Santiago, Chile. Sci. Total Environ. 512 (2015), 133–142. https://doi.org/10.1016/j.scitotenv.2015.01.006.
Whitt, W., Zhang, X., 2019. Forecasting arrivals and occupancy levels in an emergency department. Operations Research for Health Care 21, 1–18. https://doi.org/10.1016/j.orhc.2019.01.002.
Winters, P.R., 1960. Forecasting sales by exponentially weighted moving averages. Manage. Sci. 6 (3), 324–342.
Wong, P.P., Lai, P.-C., Allen, R., Cheng, W., Lee, M., Tsui, A., Tang, R., Thach, T.-Q., Tian, L., Brauer, M., et al., 2019. Vertical monitoring of traffic-related air pollution (trap) in urban street canyons of hong kong. Sci. Total Environ. 670, 696–703. https://doi.org/10.1016/j.scitotenv.2019.03.224.
World Health Organization, 2013. The United Nations Children's Fund (UNICEF), Ending Preventable Child Deaths from Pneumonia and Diarrhoea by 2025 The integrated Global Action Plan for Pneumonia and Diarrhoea (GAPPD). Tech. rep., WHO.
World Health Organization, International Statistical Classification of Diseases and Related Health Problems, 10th Revision, Tech. rep., WHO, https://icd.who.int/browse10/2016/en [Accessed: 2019/01/14] (2016)..
Zivot, E., Wang, J., 2007. Modeling financial time series with S-Plus, vol. 191. Springer Science & Business Media.